Multi-component Solute Transport Model with Cation Exchange under Redox Environment and its Application for Designing the Slow Infiltration Setup

Guerra, Gingging
Institute of Environmental Systems : Graduate Student

Jinno, Kenji
Institute of Environmental Systems : Professor

Hiroshiro, Yoshinari
Institute of Environmental Systems : Associate Professor

Nakamura, Koji
Institute of Environmental Systems : Graduate Student

出版情報：九州大学工学紀要. 64 (1), pp.79-100, 2004-03. 九州大学大学院工学研究院
バージョン：
権利関係：

Memoirs of the Faculty of Engineering, Kyushu University, Vol. 64, No. 1, March 2004

Multi-component Solute Transport Model with Cation Exchange under Redox Environment and its Application for Designing the Slow Infiltration Setup

by

Gingging GUERRA*, Kenji JINNO**, Yoshinari HIROSHIRO*** and Koji NAKAMURA*

(Received December 17, 2003)

Abstract

The present trend of disposing treated sewage water by allowing it to infiltrate the soil brings a new dimension to environmental problems. It is therefore necessary to identify the chemicals likely to be present in treated sewage water. A soil column experiment was conducted to determine the behavior of chemical species in soil columns applied with secondary treated sewage water. To predict the behavior of chemical species, a multicomponent solute transport model that includes the biochemical redox process and cation exchange process was developed. The model computes changes in concentration over time caused by the processes of advection, dispersion, biochemical reactions and cation exchange reactions. The solute transport model was able to predict the behavior of different chemical species in the soil column applied with secondary treated sewage water. The model reproduced the sequential reduction reaction. To design the safe depth of plow layer where NO_3^- is totally reduced, a numerical study of NO_3^- leach was done and it was found out that the pore velocity and concentration of CH_2O at the inject water was found to affect NO_3^- reduction in the mobile pore water phase. It is revealed that the multicomponent solute transport model is useful to design the land treatment system for NO_3 removal from wastewater.

Keywords: Biochemical redox processes, Cation exchange processes, Microbially mediated redox reactions

Nomenclature

$[C_i]_{mob}$: Concentration of chemical species i in the mobile pore water phase (mmol/L)
$[C_i]_{bio}$: Concentration of chemical species i in the bio phase (mmol/L)
$[C_i]_{mat}$: Concentration of chemical species i in the matrix phase (mmol/L)
$[C_i]_{im}$: Concentration of chemical species i in the solid phase (mmol/L)
v': Pore water velocity (cm/sec)
t : Time (sec)

*Graduate Student, Institute of Environmental Systems
**Professor, Institute of Environmental Systems
***Associate Professor, Institute of Environmental Systems

z : Distance (cm)
D : Hydrodynamic dispersion coefficient (cm^2/sec)
$S1_{(i)}$: Exchange reaction term at the concentration difference between the pore water and the biophase
$S2_{(i)}$: Exchange reaction term at the concentration difference between pore water and the soil matrix
$S3_{(i)}$: Cation exchange reaction term between the pore water and the solid phase
N : Correspond to 9 chemical species Na^+, K^+, Mg^{2+}, Ca^{2+}, Mn^{2+}, Fe^{2+}, O_2, NO_3^- and CH_2O
α : Exchange coefficient ($1\ day^{-1}$)
β : Exchange coefficient ($1\ day^{-1}$)
γ : Exchange coefficient ($1\ day^{-1}$)
θ_{bio} : Water content for bio phase
θ_w : Water content for mobile phase
θ_{mat} : Water content for matrix phase
$S3_{Fe^{2+}}$: Pore water and solid phase exchange reaction term of Fe^{2+}
K_{CH_2O} : Half velocity concentration for CH_2O (mmol/L)
K_{O_2} : Half velocity concentration for O_2 (mmol/L)
$K_{NO_3^-}$: Half velocity concentration for NO_3^- (mmol/L)
$v_{max}^{O_2}$: Maximum growth rate of aerobic Bacteria X1 ($1\ day^{-1}$)
$v_{max}^{NO_3^-}$: Maximum growth rate of anaerobic Bacteria X1 ($1\ day^{-1}$)
$v_{max}^{MnO_2}$: Maximum growth rate of Bacteria X2 ($1\ day^{-1}$)
$v_{max}^{Fe(OH)_3}$: Maximum growth rate of Bacteria X3 ($1\ day^{-1}$)
v_{X1dec} : Constant decay rate of Bacteria X1 ($1\ day^{-1}$)
v_{X2dec} : Constant decay rate of Bacteria X2 ($1\ day^{-1}$)
v_{X3dec} : Constant decay rate of Bacteria X3 ($1\ day^{-1}$)
$IC_{NO_3^-}$: Inhibition concentration of NO_3^- against O_2 (mmol/L)
$P_{Fe^{2+}}$: Production factor for Fe^{2+}
$P_{Mn^{2+}}$: Production factor for Mn^{2+}
U_{O_2} : Growth yield factor for O_2
$U_{NO_3^-}$: Growth yield factor for NO_3^-
$U_{Fe(OH)_3}$: Growth yield factor for $Fe(OH)_3$
U_{MnO_2} : Growth yield factor for MnO_2
$Y_{CH_2O}^{O_2}$: Yielding coefficient of O_2
$Y_{CH_2O}^{NO_3}$: Yielding coefficient of NO_3^-
$Y_{CH_2O}^{Fe(OH)_3}$: Yielding coefficient of $Fe(OH)_3$
$Y_{CH_2O}^{MnO_2}$: Yielding coefficient of MnO_2
f_{sl} : Slope of switch function
O_{2thres} : Threshold value of O_2 (mmol/L)
$F(O_{2bio})$: Switching function of O_2

1. Introduction

Wastewater treatment by land application has been in practice in many parts of the world because it is believed that passage through the soil environment of wastewater will provide further removal of certain chemical and microbial contaminants. The structure, chemistry and the biological activity in some soils make them ideal to treat wastewater to protect ground and surface water. Wastewater disposal on land will be a viable treatment method only if the protection of groundwater from possible degradation is held as a primary

objective (Polprasert, 1996). The present trend of disposing treated sewage water by allowing it to infiltrate the soil brings a new dimension to environmental problems. Nitrogen from such treatment systems is currently of concern because of the nitrate contamination of drinking water supplies and the eutrophication of coastal waters. Therefore it is necessary to study the governing mechanisms for the transport and fate of nitrogen and other contaminants from treated sewage water. The development and use of mathematical models provides a better understanding of the important biological, chemical and hydrological processes relevant to contaminant transport. In order to predict the effect of nitrate pollution on the long term water resource quality, models have to be constructed which both yield a quantitative explanation of the present state and predict future developments. Such models should be based on a proper understanding both of nitrate transport through aquifers and of chemical processes within aquifers that may affect nitrate concentrations. Attempts to model nitrate transport and reduction in aquifers have so far been few (Frind et al, 1990; Kinzelbach and Schäfer, 1989).

During the last decade coupled modeling of groundwater transport and chemical reaction has gone through a strong development. Models range from simple one-dimensional transport models coupled with equilibrium codes (Dance and Reardon, 1983; Appello and Willemsen, 1987) to complex two or three-dimensional models (Liu and Nasarimhan, 1989 a,b; Kinzelbach and Schäfer, 1989). Most work has been done on ion exchange processes and these models are typically validated by laboratory and field tracer experiments (Vallochi et al, 1981; Appello et al., 1990). Few models consider redox reactions (Liu and Nasarimhan, 1989 a,b) since they present an increasing numerical complexity. Kinetic reactive-transport models that have some redox capability usually in the form of biodegradation kinetics include those developed by Mc Nab and Nasarimhan (1994); Lensing et al. (1994); Schäfer and Therrien (1995).

For simulating nitrogen (N) transport and transformations, nitrification and denitrification in groundwater must be represented by kinetic expressions, which take the form of multiple nutrient Monod type equations. Several groups of researchers have recently simulated heterotrophic denitrification in one- or two- dimensional saturated groundwater flow systems. Kinzelbach et al. (1991) was able to describe the interactive transport of oxygen, nitrate, organic substrates and microbial mass in two dimensions, including the possibility of diffusion-limited exchange between different phases in the aquifer. Three model phases (mobile pore water, biophase and aquifer material) are taken into account. Lensing et al. (1994) used a multi-component transport reaction model to bacterially catalyzed redox processes. The exchange between the three different phases: pore water phase, bio phase and aquifer matrix is also considered. The sub-models are coupled with the equations of the microbially mediated redox reactions. Schäfer et al. (1998) developed the transport, biochemistry and chemistry (TBC) model that numerically solves the equations for reactive transport in three-dimensional saturated groundwater flow. Solute transport is coupled with microbially mediated organic carbon degradation. Microbial growth is assumed to follow Monod type kinetics. Schäfer et al. (1998) in his model application to a column study on organic carbon degradation considered five microbial groups in the model. The model provides a temporally and spatially resolved quantification of microbial degradation activity.

Mac Quarie et al. (2001) have presented the theory and numerical solution of a reactive transport model that is intended to represent the major flow, transport and biogeochemical processes involved in wastewater migration in a shallow aquifer. A numerical model was developed for variably saturated flow and reactive transport of multiple species. The model

suggested that adding labile organic carbon sources to septic drain fields could enhance heterotrophic denitrification and thus reduce NO_3^- concentration in shallow ground water. The simulations could help to clarify the effect of the ways of organic matter application on the process of denitrification.

Land application of treated sewage water in the paddy field has gradually become the most popular way of reuse. In a paddy field situation, successive chemical transformations occur like denitrification, oxidation and reduction (redox) reactions and cation exchange reactions. Oxidation and reduction processes exert an important control on the distribution of chemical species like O_2, NO_3^-, Mn^{2+} and Fe^{2+} etc. under natural condition in groundwater. Stumm and Morgan (1981) pointed out that the most redox processes encountered in natural aquatic systems need biological mediation. Since redox processes are always catalyzed by several microorganisms, the chemical reactions are paralleled by an ecological sequence of microorganisms. The extent and velocity of these redox reactions are strictly correlated with growth and metabolism of several microorganisms. The treatment of redox reactions as biological processes delivers the required data for kinetic approaches to model redox reactions in groundwater systems (Stumm and Morgan, 1981).

The slow rate process of treatment of wastewater is focused in this study. Slow rate process is the controlled application of wastewater to land at a rate of few centimeters of liquid per week. The flow path depends on infiltration, and usually on lateral flow within the treatment site. Treatment occurs by means of physical, chemical and biological processes at the surface and as the wastewater flow through the plant-soil matrix (Polprasert, 1996).

Nitrate is very prominent among the contaminants entering the groundwater systems from fertilization and wastewater irrigation. It is highly soluble, mobile and represents a health hazard to human infants at relatively low concentrations (Burden, R.J., 1982). The recent recognition of denitrification as an active process for the removal of nitrate from certain favorable hydrogeologic environments is an important step in the understanding of nitrate processes. Denitrification is the biologically mediated transformation of nitrate to nitrogen gas. The bacteria responsible for denitrification are facultative anaerobes that use nitrate in place of oxygen for their respiratory processes under anaerobic conditions. This transformation requires an organic carbon food source for the bacteria to metabolize and CO_2 is formed as a product of metabolism (Trudell M.R. et al, 1986).

The purpose of this study is to assess and predict the behavior of different chemical species in soil columns applied with secondary treated sewage water. A solute transport model that takes into consideration the biochemical reactions and cation exchange reactions was developed. The results of the soil column experiments were compared with the results of simulation model. It was found out that the multicomponent solute transport model was able to predict the behavior of different chemical species in the soil column applied with secondary treated sewage water, however it is necessary to determine the safe depth of the plow layer that is safe for nitrate (NO_3^-) leaching.

In this study, the numerical modeling of NO_3^- leach was done using the multicomponent solute transport model to determine the effect of the pore velocity and input CH_2O concentration needed to reduce the NO_3^- concentration. To design the depth of the plow layer that is safe for NO_3^- leaching, it is necessary to determine the depth where NO_3^- will be totally reduced. In the simulation model the input values of pore velocity and input CH_2O concentration was varied to design the safe depth of plow layer in soil columns.

2. Methodology—Soil Column Experiment

The soil column experiment was conducted using soils collected from actual paddy field and were packed in two 10 cm diameter PVC cylinder columns of different thickness of plow layers 10 cm and 20 cm respectively (**Fig. 1**). Treated sewage water was constantly supplied up to 5 cm at the top of the two soil columns in order to reproduce the redox condition similar to paddy field. **Table 1** shows the concentration of the injection water. Glass beads were used to support the plow layer in soil column at 15 cm in both soil columns. The experiment was conducted for the duration of 49 days and the average temperature was measured at 30°C. **Table 2** shows the soil properties and **Table 3** shows the chemical components of the paddy soil. Soil solution samples collected by porous cups and column outflow were analyzed for

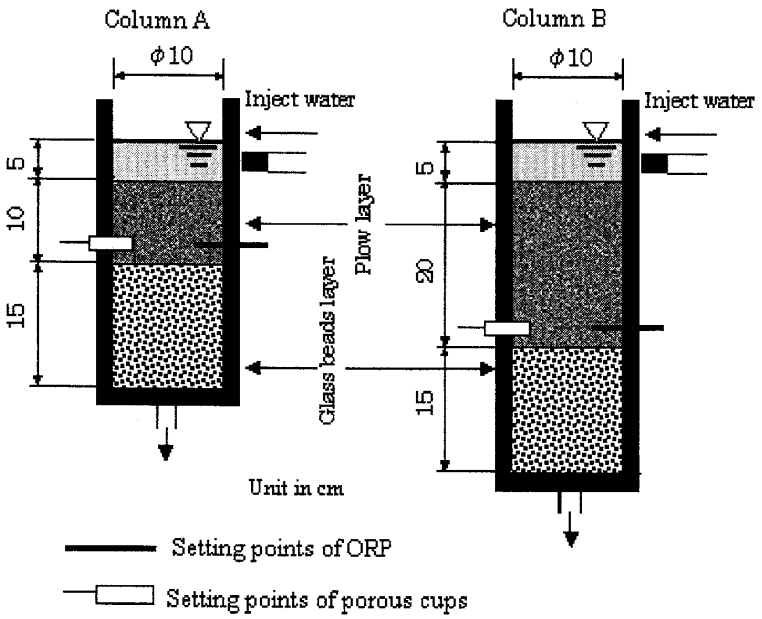

Fig. 1 Experimental column equipment.

Table 1 Concentration of injection water.

Na^+	10.146 meq/L	NH_4^+	0.432 meq/L
K^+	0.775 meq/L	NO_3^-	0.378 meq/L
Ca^{2+}	4.164 meq/L	TOC(CH_2O)	6.23 meq/L
Mg^{2+}	2.085 meq/L	EC	1.55 mS/cm
Fe^{2+}	0.066 meq/L	pH	7.2
Mn^{2+}	0.024 meq/L	Temperature	30°C

Table 2 Soil properties of paddy soil.

Cation exchange capacity	Selectivity coefficients			
CEC (mmolc/100g)	$K_{Ca/Na}$	$K_{Ca/K}$	$K_{Ca/Mg}$	$K_{Ca/Fe}$
13.52	0.453	0.0428	1.2	1.2

Table 3 Chemical component of paddy soil.

Chemical species	% composition
Fe_2O_3	5.34
MnO_2	0.05
Al_2O_3	8.09
SiO_2	77.58
CH_2O	6.08
C	1.96
H	0.76
N	0.15
Total	100.01

Na^+, K^+, Mg^{2+}, Ca^{2+}, Mn^{2+}, Fe^{2+}, NH_4^+-N and NO_3^--N concentrations. EC (Electrical Conductivity), pH and ORP (Oxidation Reduction Potential) were also measured.

3. The Multi-component Solute Transport Model Conceptual Model

The biochemical and chemical model (**Fig.2**) describes the interaction of O_2, NO_3^-, CH_2O, bacteria, MnO_2, $Fe(OH)_3$, Na^+, K^+, Mg^{2+}, Ca^{2+}, Mn^{2+} and Fe^{2+}. This model takes into account the microbially mediated redox reaction and the cation exchange reaction. It also takes into consideration the four different model phases: mobile pore water phase, immobile biophase, solid matrix phase and solid phase. The bacteria are assumed to reside in the immobile biophase. Exchange processes are considered between the different model phases. The exchange between two phases is modeled by a linear exchange term. Mass exchange of dissolved species is governed by the concentration difference of the species in the pore water phase $[C_i]_{mob}$, the bio phase $[C_i]_{bio}$, the matrix phase $[C_i]_{mat}$ and the exchange coefficients

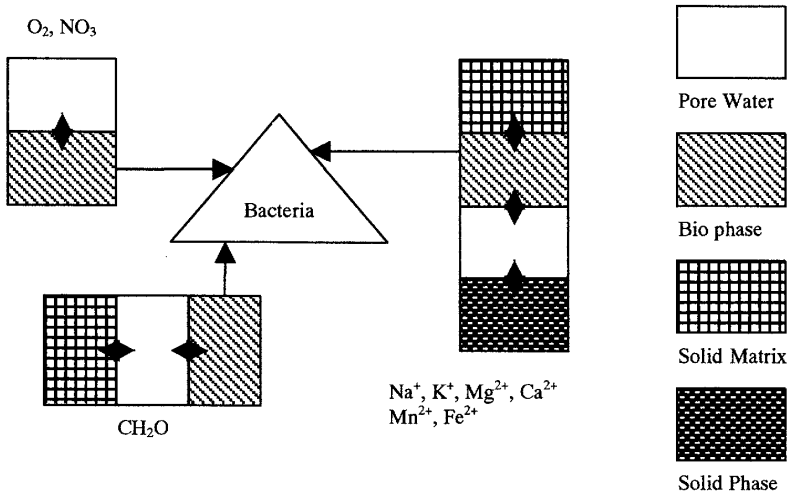

Fig. 2 Scheme of biochemical model.

α and β. This model belongs to the biofilm models, where microorganisms are assumed to reside in the immobile biophase. The biofilm model assumes microbes distribute themselves uniformly over the soil particles creating a film. Internal diffusion limits the transport of substrate and contaminants to the microbes in the film. In most biofilm models, a direct exchange between the biophase and the aquifer material is not considered (Schäfer et al., 1998).

4. Theoretical Model Development—Reactive Solute Transport Model

The one-dimensional partial differential equation governing the convective-dispersive solute transport of chemical species i considering biochemical and chemical reactions in a sub-aqueous soil can be written as: (Bear, 1972; Lensing, et al., 1994; Hiroshiro et al., 1999)

$$\frac{\partial}{\partial t}(\theta_w[C_i]_{mob})+\frac{\partial}{\partial x}(\theta_w v'[C_i]_{mob})=\frac{\partial}{\partial x}\left(\theta_w D\frac{\partial[C_i]_{mob}}{\partial x}\right)+\theta_w S1_{(i)}+\theta_w S2_{(i)}+\theta_w S3_{(i)} \quad (1)$$

where i is the chemical species given by i=1, 2, 3, 4, 5, 6, 7, 8, and 9 correspond to Na^+, K^+, Mg^{2+}, Ca^{2+}, Mn^{2+}, Fe^{2+}, O_2, NO_3^- and CH_2O, respectively. C_i is the concentration of chemical species i in the pore water (mmol l^{-1}), v' is pore water velocity (cm sec^{-1}), t is time (sec), x is distance, D is the hydrodynamic dispersion coefficient (cm^2 sec^{-1}). $S1_{(i)}$, $S2_{(i)}$ and $S3_{(i)}$ are the chemical sink/source term representing the exchange with other phases and the chemical and biochemical reactions (mmol $l^{-1}sec^{-1}$) and formulated as follows:

$$\theta_w S1_{(i)}=\frac{\alpha\theta_{bio}\theta_w}{\theta_{bio}+\theta_w}([C_i]_{bio}-[C_i]_{mob}) \quad (2)$$

$$\theta_w S2_{(i)}=\frac{\beta\theta_{mat}\theta_w}{\theta_{mat}+\theta_w}([C_i]_{mat}-[C_i]_{mob}) \quad (3)$$

$$\theta_w S3_{(i)}=-\frac{\partial}{\partial t}(\theta_w[C_i]_{im}) \quad (4)$$

where $S1_{(i)}$ is the exchange rate at the concentration difference between the pore water and the biophase, $S2_{(i)}$ is the exchange rate at the concentration difference between pore water and the soil matrix, and $S3_{(i)}$ is the cation exchange reaction rate between the pore water and the solid phase. $[C_i]_{mob}$, $[C_i]_{bio}$, $[C_i]_{mat}$ and $[C_i]_{im}$ correspond to the concentration of chemical species (mmol l^{-1}) in the pore water, the biophase, the soil matrix, and the solid phase, respectively. α and β are the exchange coefficients. In equations (2) and (3) the theory of mass transport at the boundary of film interface is applied. The biophase is conceptualized as an operative means to easily include diffusion limited exchange process between the mobile pore water and bacteria. The diffusion limitation can be due either to microscale (or real biofilm) diffusion or to limited macroscale exchange between different zones of the aquifer. This diffusional transfer can be represented by mass transport exchange coefficients α and β (Kinzelbach et al, 1991). The chemical species considered in the model are summarized in **Table 4**. Each chemical species requires an equation in the form of equilibrium equations. The formulation of equilibrium equations results in a highly non-linear

Table 4 Chemical species considered in the model.

Pore water	Na^+_{mob} K^+_{mob} Mg^{2+}_{mob} Ca^{2+}_{mob} Mn^{2+}_{mob} Fe^{2+}_{mob} $O_{2\,mob}$ $NO_3^-{}_{mob}$ CH_2O_{mob}
Bio Phase	$O_{2\,bio}$ $NO_3^-{}_{bio}$ Mn^{2+}_{bio} Fe^{2+}_{bio} CH_2O_{bio} MnO_{2bio} $Fe(OH)_{3bio}$
Solid Phase	Na^+_{im} K^+_{im} Mg^{2+}_{im} Ca^{2+}_{im} Mn^{2+}_{im} Fe^{2+}_{im}
Soil matrix	CH_2O_{mat} MnO_{2mat} $Fe(OH)_{3mat}$
Bacteria	X1 X2 X3

partial differential equations.
For the chemical species related to Fe^{2+} the following equations are formulated:
Biophase:

$$Fe^{2+}: \frac{\partial}{\partial t}(\theta_{bio}[Fe^{2+}]_{bio}) = \frac{\theta_{bio}}{P_{Fe^{2+}}}\left[\frac{\partial X3}{\partial t}\right]_{Iron} - \frac{\alpha\theta_{bio}\theta_w}{\theta_{bio}+\theta_w}([Fe^{2+}]_{bio}-[Fe^{2+}]_{mob}) \tag{5}$$

$$Fe(OH)_3: \frac{\partial}{\partial t}(\theta_{bio}[Fe(OH)_3]_{bio}) = -\frac{\theta_{bio}}{U_{Fe(OH)_3}}\left[\frac{\partial X3}{\partial t}\right]_{grow} - \frac{\gamma\theta_{bio}\theta_{mat}}{\theta_{bio}+\theta_{mat}}([Fe(OH)_3]_{bio}-[Fe(OH)_3]_{mat}) \tag{6}$$

Pore water phase:

$$Fe^{2+}: \frac{\partial}{\partial t}(\theta_w[Fe^{2+}]_{mob}) + \frac{\partial}{\partial t}(\theta_w v'[Fe^{2+}]_{mob}) = \frac{\partial}{\partial t}\left(\theta_w D\frac{\partial[Fe^{2+}]_{mob}}{\partial x}\right) + \frac{\alpha\theta_{bio}\theta_w}{\theta_{bio}+\theta_w}([Fe^{2+}]_{bio}-[Fe^{2+}]_{mob}) + \theta_w S3_{Fe^{2+}} \tag{7}$$

Solid Phase:

$$Fe^{2+}: \frac{\partial}{\partial t}(\theta_w[Fe^{2+}]_{im}) = -\theta_w S3_{Fe^{2+}} \tag{8}$$

Soil Matrix:

$$Fe(OH)_3: \frac{\partial}{\partial t}(\theta_{mat}[Fe(OH)_3]_{mat}) = \frac{\gamma\theta_{bio}\theta_{mat}}{\theta_{bio}+\theta_{mat}}([Fe(OH)_3]_{bio}-[Fe(OH)_3]_{mat}) \tag{9}$$

Bacteria:

$$X3: \left[\frac{\partial X3}{\partial t}\right]_{Total-Growth} = \left[\frac{\partial X3}{\partial t}\right]_{grow} + \left[\frac{\partial X3}{\partial t}\right]_{decay} \tag{10}$$

$$X3: \left[\frac{\partial X3}{\partial t}\right]_{grow} = \nu_{\max}^{Fe(OH)_3} \cdot \frac{IC_{NO_3^-}}{IC_{NO_3^-}+[NO_3^-]_{bio}} \cdot \frac{[CH_2O]_{bio}}{K_{CH_2O}+[CH_2O]_{bio}} \cdot \frac{[Fe(OH)_3]_{bio}}{K_{Fe(OH)_3}+[Fe(OH)_3]_{bio}} \cdot X3 \tag{11}$$

$$\left[\frac{\partial X3}{\partial t}\right]_{decay} = -\nu_{X3dec} \cdot X3 \tag{12}$$

where α, γ are the exchange coefficients, θ_{bio}, θ_w, and θ_{mat} correspond to water content for bio phase, mobile phase and matrix phase respectively, $P_{Fe^{2+}}$ is the production factor for Fe^{2+}, $U_{Fe(OH)_3}$ is the growth yield factor for $Fe(OH)_3$, $S3_{Fe^{2+}}$ is the pore water and solid phase exchange reaction term of Fe^{2+}, $IC_{NO_3^-}$ is the inhibition concentration of NO_3^- against O_2, K_{CH_2O} is the half velocity concentration for CH_2O, $\nu_{\max}^{Fe(OH)_3}$ is the maximum growth rate of bacteria X3 and ν_{X3dec} is the constant decay rate of bacteria X3.

5. Bacteria Growth

The modeling of complex redox sequences requires the consideration of different metabolisms. It also requires the consideration of a variety of substrates, including organic compounds, O_2, NO_3^-, MnO_2 and $Fe(OH)_3$. Since each mode of energy metabolism is associated with a different functional bacterial group, the growth of each group must be considered in the model (Kindred and Celia, 1989). In this model the three functional bacterial groups, bacteria X1, X2 and X3 that are assumed to reside in the immobile biophase are considered. **Table 5** shows the sequential redox chemical reaction of bacteria X1, X2 and X3. In the model, the bacteria group X1 uses under aerobic conditions, molecular oxygen and under denitrifying conditions, NO_3^- as electron acceptor. Bacteria X2 uses MnO_2 while bacteria X3 uses $Fe(OH)_3$ as electron acceptor. The microorganisms use dissolved organic carbon chemically defined as CH_2O and the utilizable portion of dead bacteria of 90% as their substrate. Bacteria X1, X2 and X3 oxidizes CH_2O to CO_2 in the model.

Table 5 Chemical reactions of bacteria.

Bacteria	Reaction
Aerobic X1	$CH_2O+O_2 \Rightarrow CO_2+H_2O$
Denitritying X1	$CH_2O+4/5NO_3^-+4/5H^+ \Rightarrow CO_2+2/5N_2+7/5H_2O$
Manganese reducing X2	$CH_2O+2MnO_2+4H^+ \Rightarrow 2Mn^{2+}+3H_2O+CO_2$
Iron reducing X3	$CH_2O+4Fe(OH)_3+8H^+ \Rightarrow 4Fe^{2+}+11H_2O+CO_2$

Attached bacteria have an advantage over suspended bacteria and dominate the heterotrophic degradation of dissolved organic carbon (Bouwer and Cobb, 1987). Their uptake of substrate and electron acceptors takes place only via the immobile water phase. Though existing in real aquifers, mobile bacteria are not considered in the model.

In aerobic parts of aquifers the microbial population is usually dominated by heterotrophic bacteria. This bacteria uses dissolved organic carbon as energy and carbon source and molecular oxygen as electron acceptor. Further heterotrophic metabolisms using other electron acceptors are suppressed by the presence of oxygen. Some aerobic bacteria are capable of nitrate-reducing metabolism. The necessary enzymes are not maintained and are induced by low oxygen concentrations (Bouwer and Cobb, 1987). The growth and metabolism of different groups of microbial populations in the immobile biophase is based on Monod kinetics and are formulated as follows:

$$X1:\left[\frac{\partial X1}{\partial t}\right]_{Total\_Growth}=\left[\frac{\partial X1}{\partial t}\right]_{aerobic\_condition}+\left[\frac{\partial X1}{\partial t}\right]_{denitrifying\_condition}+\left[\frac{\partial X1}{\partial t}\right]_{decay} \tag{13}$$

$$\left[\frac{\partial X1}{\partial t}\right]_{aerobic\_condition}=v_{\max}^{O_2}\cdot\{1-F(O_{2bio})\}\cdot\frac{[CH_2O]_{bio}}{K_{CH_2O}+[CH_2O]_{bio}}\cdot\frac{[O_2]_{bio}}{K_{O_2}+[O_2]_{bio}}\cdot X1 \tag{14}$$

$$\left[\frac{\partial X1}{\partial t}\right]_{denitrifying\_condition}=v_{\max}^{NO_3^-}\cdot\{F(O_{2bio})\}\cdot\frac{[CH_2O]_{bio}}{K_{CH_2O}+[CH_2O]_{bio}}\cdot\frac{[NO_3^-]_{bio}}{K_{NO_3^-}+[NO_3^-]_{bio}}\cdot X1 \tag{15}$$

$$\left[\frac{\partial X1}{\partial t}\right]_{decay}=-v_{X1dec}\cdot X1 \tag{16}$$

$$X2:\left[\frac{\partial X2}{\partial t}\right]_{grow}=v_{\max}^{MnO_2}\cdot\frac{IC_{NO_3^-}}{IC_{NO_3^-}+[NO_3^-]_{bio}}\cdot\frac{[CH_2O]_{bio}}{K_{CH_2O}+[CH_2O]_{bio}}\cdot\frac{[MnO_2]_{bio}}{K_{MnO_2}+[MnO_2]_{bio}}\cdot X2 \tag{17}$$

$$\left[\frac{\partial X2}{\partial t}\right]_{decay}=-v_{X2dec}\cdot X2 \tag{18}$$

$$X3:\left[\frac{\partial X3}{\partial t}\right]_{Total\_Growth}=\left[\frac{\partial X3}{\partial t}\right]_{grow}+\left[\frac{\partial X3}{\partial t}\right]_{decay} \tag{19}$$

$$X3:\left[\frac{\partial X3}{\partial t}\right]_{grow}=v_{\max}^{Fe(OH)_3}\cdot\frac{IC_{NO_3^-}}{IC_{NO_3^-}+[NO_3^-]_{bio}}\cdot\frac{[CH_2O]_{bio}}{K_{CH_2O}+[CH_2O]_{bio}}\cdot\frac{[Fe(OH)_3]_{bio}}{K_{Fe(OH)_3}+[Fe(OH)_3]_{bio}}\cdot X3 \tag{20}$$

$$\left[\frac{\partial X3}{\partial t}\right]_{decay}=-v_{X3dec}\cdot X3 \tag{21}$$

$$F(O_{2bio})=0.5-\frac{1}{\pi}\tan^{-1}[O_{2bio}-O_{2thres})f_{sl}] \tag{22}$$

where X1, X2 and X3 correspond to the concentration of O_2 and NO_3^-, MnO_2 and $Fe(OH)_3$ reducing bacteria, $v_{\max}^{O_2}$, $v_{\max}^{NO_3^-}$, $v_{\max}^{MnO_2}$ and $v_{\max}^{Fe(OH)_3}$ correspond to the maximum growth rate of O_2, NO_3^-, MnO_2 and $Fe(OH)_3$ reducing bacteria, v_{X1dec}, v_{X2dec} and v_{X3dec} correspond to the constant decay rate of bacteria X1, X2 and X3, $F(O_{2bio})$ is the switching function parameter, O_{2thres} is the threshold concentration of O_2, f_{sl} is the slope of switch function, $[O_2]_{bio}$, $[NO_3^-]_{bio}$ and $[CH_2O]_{bio}$ correspond to concentration of O_2, NO_3^- and CH_2O in the bio phase. K_{O_2}, $K_{NO_3^-}$ and

K_{CH_2O} correspond to half velocity concentration of O_2, NO_3^- and CH_2O in the bio phase.

The bacteria are assumed to consume dissolved oxygen (DO) as long as it is available and then switch to nitrate as electron acceptor. The switching between aerobic and denitrifying growth conditions is based on the assumption of a non-competitive inhibition and is realized by a weighting function $F(O_{2bio})$ dependent on the oxygen concentration, which was developed and tested by Kinzelbach, et al. (1991). Equation (22) is based on the assumption that the same microorganisms are capable of either aerobic or denitrifying growth, depending on the oxygen concentration in their nearby environment. It allows adjustment of two characteristic features of the microbial switching, the slope f_{sl} and the threshold concentration of oxygen O_{2thres}, according to laboratory or field measurements. It is also assumed that the functional bacterial group X1 reduces nitrate quantitatively to N_2 under anaerobic conditions. This biochemical model is mathematically similar to other models that use Monod type kinetics to describe microbial activity (e.g. Schäfer et al., 1998; Widdowson et al., 1998; Kinzelbach et al., 1991; Kindred and Celia, 1989).

6. Modelling Methodology

The one-dimensional solute transport equation is solved for each chemical species. The model couples the flow equation with the solute-transport equation. The flow and transport equation are discretized using a rectangular, uniformly spaced, block centered, finite difference grid. Since artificial oscillation and numerical dispersion are encountered in the finite difference method when applied to advection-dominated problem, the method of characteristics (MOC) was used to eliminate numerical dispersion (Zheng and Bennett, 1995). The iterative numerical procedure employed for coupling of physical transport and chemical processes was based on Momii et al. (1997). The multicomponent solute transport model is applicable for one-dimensional problem involving steady-state flow. The model computes changes in concentration over time caused by the processes of advection, dispersion, cation exchange reactions and biochemical reactions.

7. Parameter Estimation

The modelling of multicomponent solute transport with biochemical reaction processes is complex because it involves specification of many biochemical parameters. Monod kinetic parameters for heterotrophic processes were selected following a review of several studies related to wastewater treatment modeling and simulation of denitrification in groundwater (Kinzelbach et al, 1991; Lensing et al, 1994; Schäfer et al, 1998; Hiroshiro et al, 1999). **Table 6** shows the different biochemical parameters used in the solute transport model. In general these parameters are affected by temperature. The temperature effect on the denitrification rate is an important feature in the design of denitrification process. Carrerra et al. (2003) studied the influence of temperature on denitrification of an industrial high-strength nitrogen wastewater in a two-sludge system and found out that the maximum denitrification rate is much higher at 25°C. The most favorable temperature for denitrification ranges from 20°C to 30°C and the average temperature measured in the present experiment is high enough at 30°C. Consequently, the parameters adjusted for this particular simulation may be the case for the most desirable denitrification. In this study, the maximum growth rate of bacteria X1, $v_{max}^{O_2}$ and $v_{max}^{NO_3^-}$ was calibrated by trial and error method until the O_2 and NO_3^- in the simulation model fit the measured concentration of O_2 and NO_3^-.

Table 6 Parameters used for the simulation.

Specific volume of biophase (n_{bio})	0.02
Specific volume of mobile phase (n_{mob})	0.48
Specific volume of matrix phase (n_{mat})	0.50
Exchange coefficient (α)	50 day^{-1}
Exchange coefficient (β)	0.005 day^{-1}
Exchange coefficient (γ)	0.00005 day^{-1}
Switching function parameter $F(O_{2bio})$	
Threshold concentration of O_2 (O_{2thres})	0.015 mmol/l
Slope of switch function (f_{sl})	40
Inhibition Constant $IC_{NO_3^-}$	0.01 mmol/l
Half velocity concentration, K	
Half velocity concentration of O_2, K_{O_2}	0.001 mmol/l
Half velocity concentration of NO_3^-, $K_{NO_3^-}$	0.001 mmol/l
Half velocity concentration of MnO_2, K_{MnO_2}	0.001 mmol/l
Half velocity concentration of $Fe(OH)_3$, $K_{Fe(OH)_3}$	0.001 mmol/l
Half velocity concentration of CH_2O, K_{CH_2O}	0.10 mmol/l
X1 - Oxygen Reducing Bacteria	
Yield Coefficient $Y_{CH_2O}^{O_2}$	0.1 mmol cell-C/mol OC
Maximum growth rate $v_{max}^{O_2}$	5.0 day^{-1}
Constant decay rate $v_{X1_{dec}}$	0.75 day^{-1}
X1 - Nitrate Reducing Bacteria	
Yield Coefficient $Y_{CH_2O}^{NO_3}$	0.081 mmol cell-C/mol OC
Maximum growth rate $v_{max}^{NO_3^-}$	4.05 day^{-1}
Constant decay rate $v_{X1_{dec}}$	0.75 day^{-1}
X2 - Manganese Reducing Bacteria	
Yield Coefficient $Y_{CH_2O}^{MnO_2}$	0.015 mmol cell-C/mol OC
Maximum growth rate $v_{max}^{MnO_2}$	0.75 day^{-1}
Constant decay rate $v_{X2_{dec}}$	0.113 day^{-1}
X3 - Iron Reducing Bacteria	
Yield Coefficient $Y_{CH_2O}^{Fe(OH)_3}$	0.01 mmol cell-C/mol OC
Maximum growth rate $v_{max}^{Fe(OH)_3}$	0.50 day^{-1}
Constant decay rate $v_{X3_{dec}}$	0.075 day^{-1}
Soil properties	
Porosity	0.48
Dispersivity α_L	0.01 cm
CEC	13.52 mmolC/100g
Selectivity Coefficients	
$K_{Ca/Mg}$	1.2 mmol/L
$K_{Ca/Mn}$	1.2 mmol/L
$K_{Ca/Fe}$	1.2 mmol/L
$K_{Ca/Na}$	0.453 mmol/L
$K_{Ca/K}$	0.0428mmol/L

8. Results and Discussions

8.1 Flow rate and permeability

Figure 3 shows the flow rate in Column A and Column B are rapidly decreasing during the first ten days and then after ten days the flow rate in Column A is almost the same with the flow rate in Column B. The average velocity was obtained by dividing the flow rate by the surface area of the column. It was assumed that the steady state was attained at the flow rate of 40 ml/day. Then the pore water velocity was determined by dividing the average velocity by porosity. In the simulation model the pore water velocity was assumed constant ($VK=7.68\times10^{-6}$ cm/sec) since the model considered only the reduced layer that is saturated. **Figure 4** shows the permeability in Column A and Column B are rapidly decreasing during the first two days and then after ten days the permeability in Column A is almost the same with the permeability in Column B. The rapid decrease in permeability could be due to clogging of the soil pores as a result of the growth of bacteria. From the experimental results of flow rate and permeability, there is no significant difference between Column A and Column B. Similar results can be expected with the two soil columns.

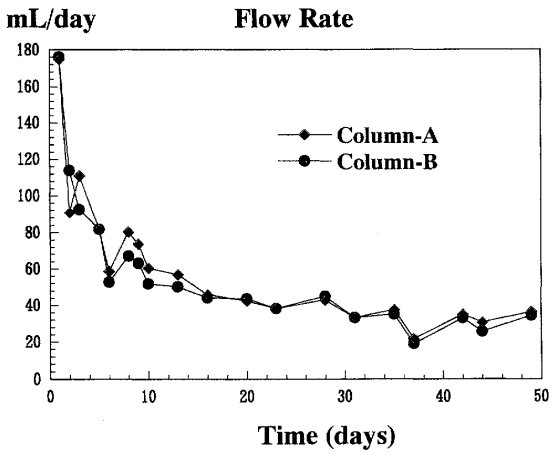

Fig. 3 Flow rate in Columns A and B.

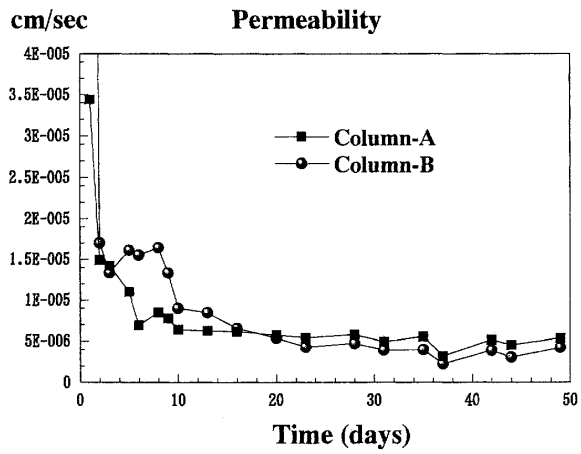

Fig. 4 Permeability in Columns A and B.

8.2 Simulation result of Dissolved Oxygen, NO_3^- and CH_2O

Figure 5 shows the simulation result of DO concentration at the top 5 cm of plow layer in the mobile phase at the early stage. DO concentration reduced at the top 0.5 cm of the column where DO concentration decreased to zero after 30 hours. **Figure 6** shows the simulation result of NO_3^- concentration in the mobile phase in the column. Denitrification occurred immediately at the top 0.5 cm of the column where NO_3^- concentration was reduced to zero after 31 hours, following the reduction of DO. **Figure 7** shows the vertical distribution of CH_2O concentration. CH_2O concentration decreased only at the top 2 cm of the column and then increased near to original concentration. CH_2O concentration degradation is relatively fast at the top 2 cm of the column, where O_2 concentration is readily available. On the other hand, CH_2O degradation is very slow at the deeper downstream of the column where both O_2 and NO_3^- concentration are very small.

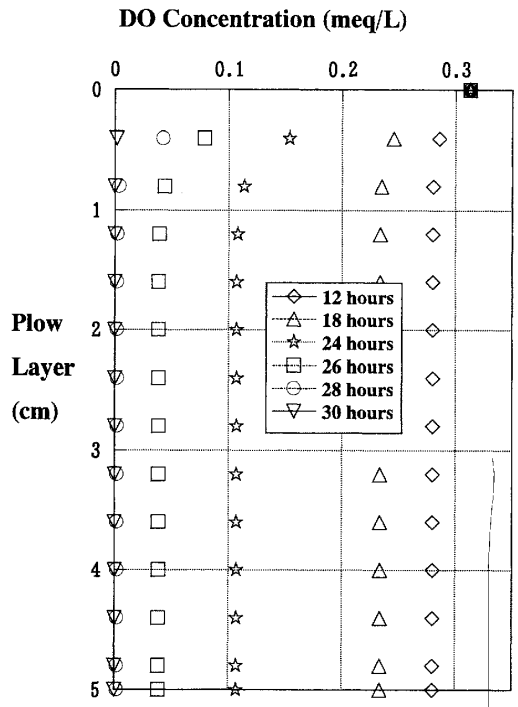

Fig. 5 Simulation result of DO concentration in the column.

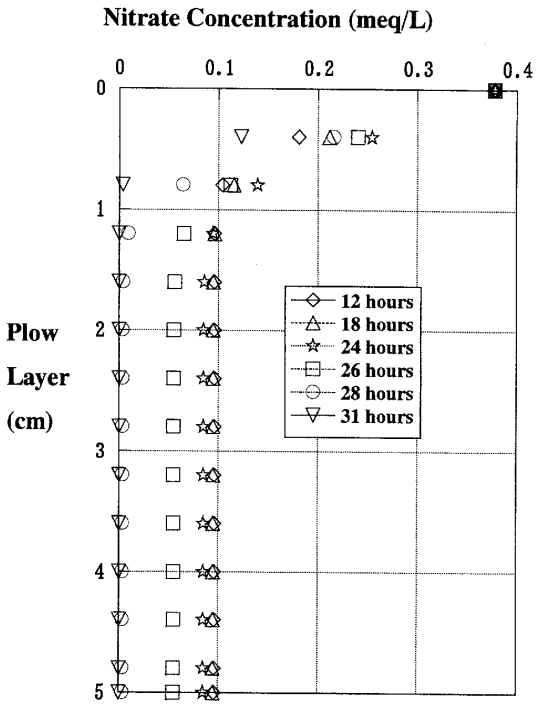

Fig. 6 Simulation result of NO_3^- concentration in the column.

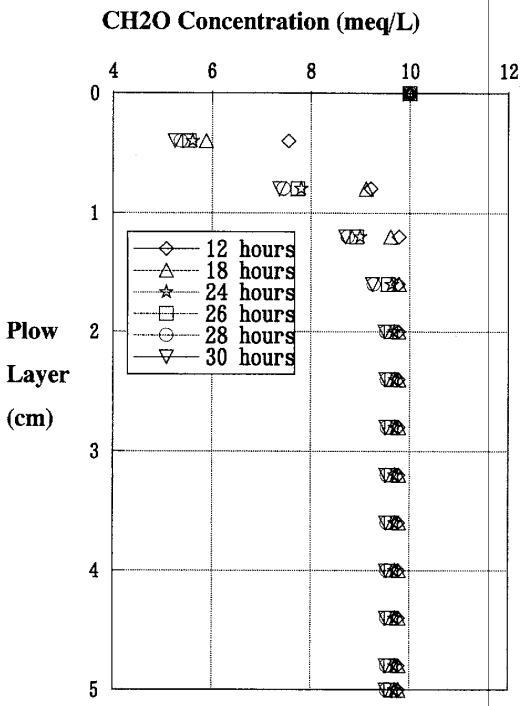

Fig. 7 Simulation result of CH_2O concentration in the column.

8.3 Comparison of observed and calculated concentration

The multicomponent solute transport model was tested by comparing the simulation results with the results of the soil column experiment by using the concentration of inject water from the soil column experiment (**Table 1**) as the concentration of inject water in the simulation model. It was found out that the multicomponent solute transport model was able to predict the behavior of different chemical species in the soil column applied with secondary treated sewage water. **Figure** 8 shows the observed cation concentration correlated fairly well with the calculated cation concentrations. K^+ concentration showed almost constant values. Na^+ concentration decreased while $Ca^{2+}$and Mg^{2+} concentrations increased at the depth 17 cm and depth 20 cm of the column due to desorption of Ca^{2+} and Mg^{2+} by Mn^{2+} and Fe^{2+}. **Figure 9** shows the comparison of observed and calculated concentrations of NO_3^-, Mn^{2+} and Fe^{2+}. NO_3^- concentration rapidly decreased at the depth 17 cm due to denitrification while Mn^{2+} and Fe^{2+} concentration increased due to dissolution from MnO_2 and $Fe(OH)_3$ during infiltration through the plow layer. These changes in concentration indicated that chemical reactions had occurred in all parts of the column.

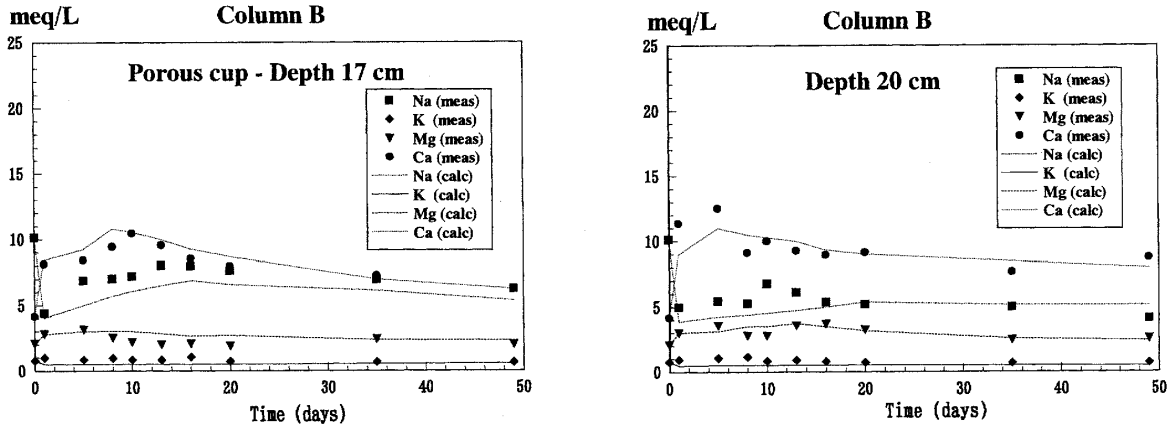

Fig. 8 Comparison of observed and calculated cation concentration in the mobile phase.

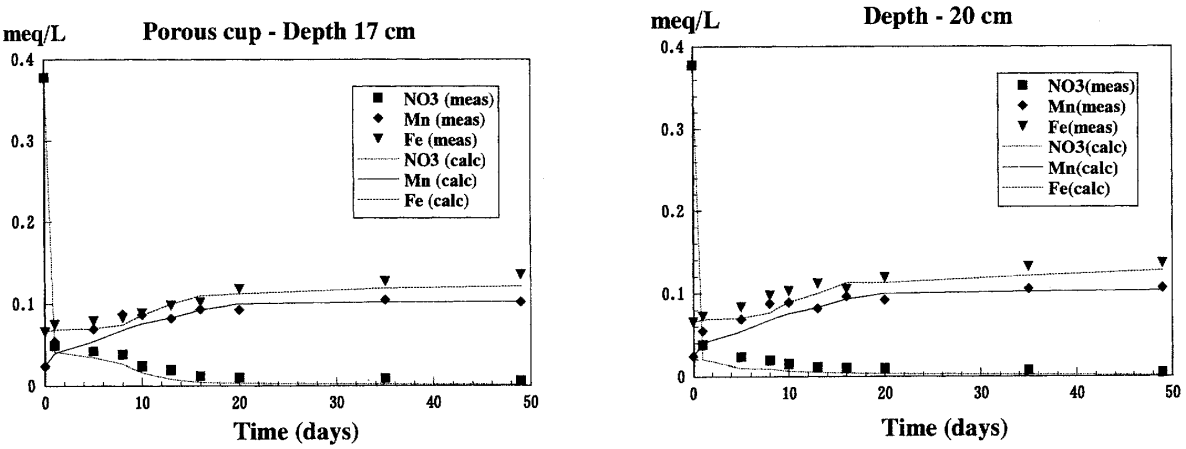

Fig. 9 Comparison of observed and calculated NO_3^-, Mn^{2+} and Fe^{2+} concentration.

8.4 Simulation result of CH_2O, MnO_2 and $Fe(OH)_3$ concentration in the biophase

Figure 10 shows the simulation results of the temporal variation of CH_2O, MnO_2 and $Fe(OH)_3$ in the biophase. CH_2O concentration decreased during the first 5 days while MnO_2 and $Fe(OH)_3$ decreased after 5 days due to consumption of bacteria. **Figure 11** shows the simulation results of the temporal variation of X1, X2 and X3 bacteria concentration at different depths in the biophase. The maximum growth of bacteria X1 occurred at the depth 5 cm of the column, where high concentrations of O_2, NO_3^- and CH_2O are present. Bacteria X1 increases rapidly during the first 5 days due to presence of O_2, NO_3^- and CH_2O concentration at the top 5 cm of the column then decreases rapidly due to decreased O_2 and NO_3^-. Bacteria X2 and X3 increase after 5 days and then decrease gradually. Bacteria X3 increases higher than bacteria X2 due to higher concentration of $Fe(OH)_3$ than MnO_2 in the matrix phase and consequently in the biophase.

The result of the soil column experiment and the solute transport model produced interesting observations on the behavior of chemical species present in the secondary treated sewage water. The result of the numerical simulation approximately agreed with the experimental results.

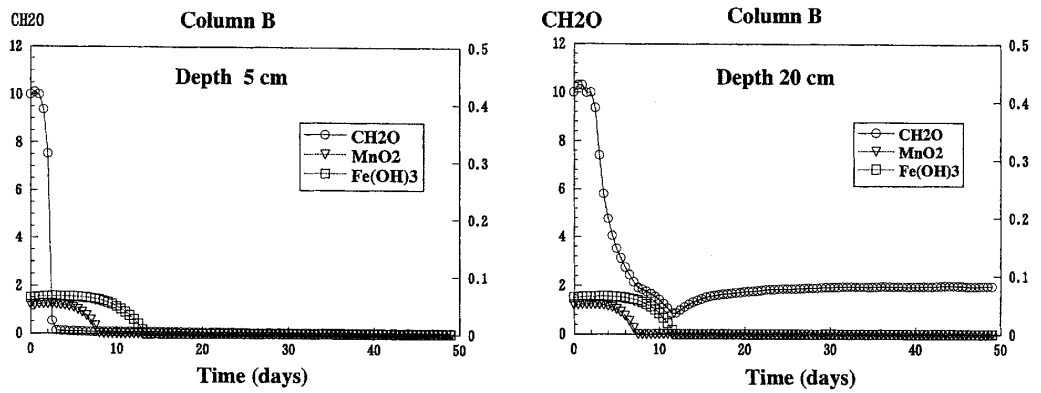

Fig. 10 Temporal variation of CH_2O, MnO_2 and $Fe(OH)_3$ at different depths in the biophase.

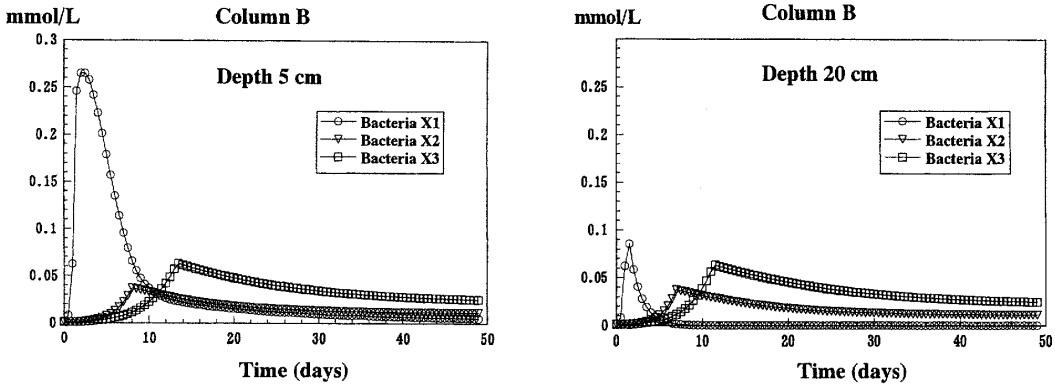

Fig. 11 Temporal variation of bacteria concentration at different depths in the biophase.

9. Design of Infiltration Treatment

In order to design the thickness of plow layer that is safe for nitrate leaching, it is necessary to determine the depth where denitrification occurs. Denitrification has been inferred from the observation of decreasing NO_3^- concentration and corresponding decline in dissolved oxygen concentration. Reduction of NO_3^- to N_2 by organic matter under anoxic conditions as a result of denitrification in soils is well documented. A number of studies (Trudell et al., 1986; Mac Quarrie et al., 2001) have shown that reduction of NO_3^- by organic matter oxidation can be important in aquifers. Accordingly Kinzelbach and Schäfer (1989) model NO_3^- reduction by organic matter in a sandy aquifer using the kinetic approach and found that the field data are well described by reaction of NO_3^- with degradable organic matter in sediments.

The design of infiltration treatment is also primarily affected by the application rate. In rapid infiltration systems, the required treatment performance is of primary importance in determining the application rate. Lance and Gerba (1977) showed that decreasing the application rate from the hydraulic limit could result in increased removals of constituents, especially NO_3^-. Since the chief mechanism of NO_3^- removal in rapid infiltration systems is denitrification and denitrification requires adequate detention time, anoxic conditions and adequate organic carbon to drive the reaction. The reduction in application rate increases detention time and increases the potential for denitrification.

In this chapter the design of infiltration treatment considered both the effect of pore velocity and input CH_2O concentration. The design of the thickness of plow layer is important in land treatment system design and operation, so as to maximize land treatment efficiency and minimize operation and maintenance costs.

9.1 Effect of pore velocity *VK* on NO_3^- leaching

Figure 12 shows the concentration of O_2, NO_3^- and CH_2O at different depths of the column when $VK=7.68\times10^{-6}$ cm/sec and the input CH_2O was 6.23 mmol/L in the simulation model. NO_3^- concentration was totally reduced after 2 days at all depths of the column. O_2 and NO_3^- concentration were reduced due to consumption of bacteria X1. **Figure 13** shows the concentration of O_2, NO_3^- and CH_2O at different depths of the column when $VK=3.84\times10^{-5}$ cm/sec and the input CH_2O at 6.23 mmol/L in the simulation model. When pore velocity $VK=3.84\times10^{-5}$ cm/sec, NO_3^- concentration decreased after 2 days then increased after 4 days at depths 5 cm and 10 cm of the column. NO_3^- concentration infiltrated deeper down to depth 10 cm due to high velocity and lack of CH_2O concentration to reduce NO_3^-. Since CH_2O induces heterotrophic denitrification, in which bacteria in anaerobic environment uses NO_3^- as electron acceptor to oxidize dissolved CH_2O. Low concentration of CH_2O will result to NO_3^- infiltration.

9.2 Effect of inject CH_2O concentration

Figure 14 shows the concentration of O_2, NO_3^- and CH_2O at different depths of the column when the input CH_2O is 0.623 mmol/L and pore velocity $VK=7.68\times10^{-6}$ cm/sec. Again NO_3^- concentration decrease after 2 days then increase after 4 days at depths 5 cm and 10 cm of the column. NO_3^- concentration infiltrated deeper down to depth 10 cm due to lack of CH_2O concentration to reduce NO_3^-. Since CH_2O induces denitrification, low concentration of CH_2O will result to NO_3^- infiltration. **Figure 15** shows the concentration of O_2, NO_3^- and CH_2O at different depths of the column when input CH_2O is 62.3 mmol/L and pore velocity

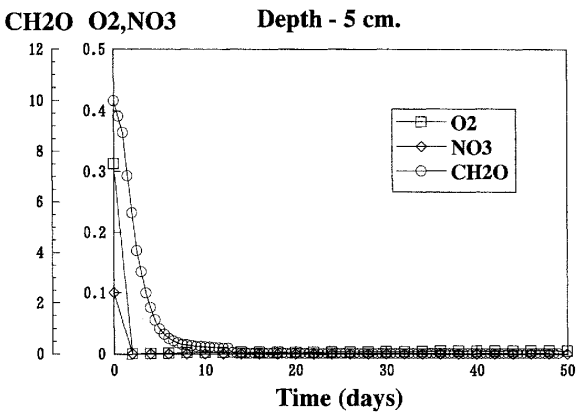

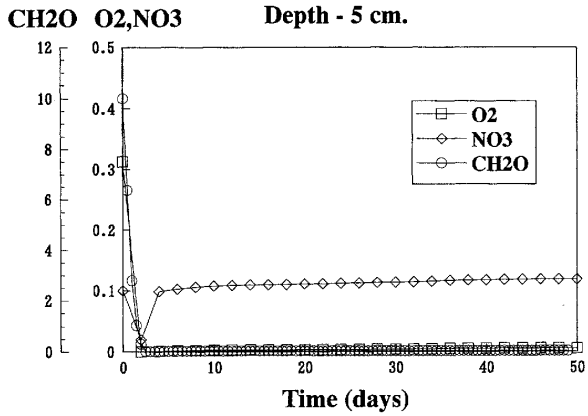

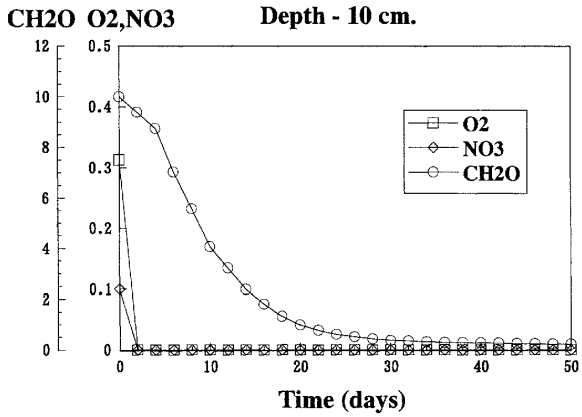

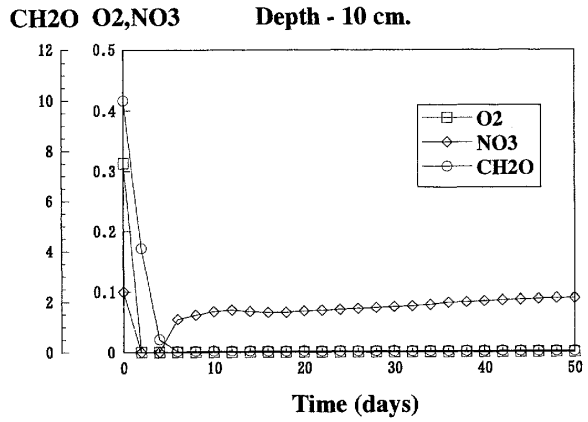

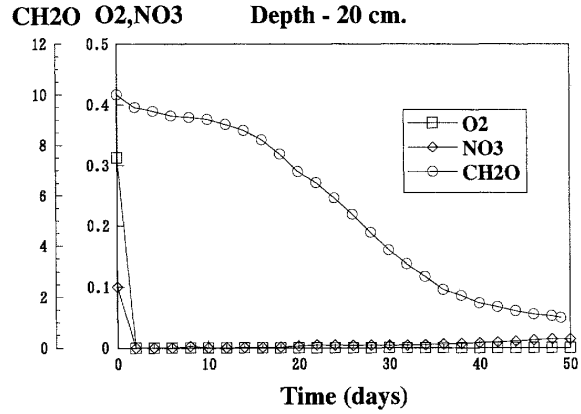

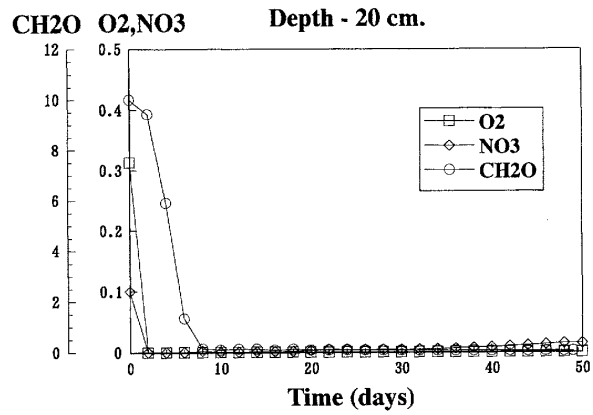

Fig. 12 Mobile redox concentration at different depths when pore velocity $VK=7.68\times10^{-6}$ cm/sec and input $CH_2O=6.23$ mmol/L.

Fig. 13 Mobile redox concentration at different depths when pore velocity $VK=3.84\times10^{-5}$ cm/sec and input $CH_2O=6.23$ mmol/L.

is $VK=7.68\times10^{-6}$ cm/sec. NO_3^- concentration was totally reduced at all depths of the column due to sufficient CH_2O concentration. CH_2O enhanced heterotrophic denitrification, in which bacteria in anaerobic environment uses NO_3^- as electron acceptor to oxidize dissolved CH_2O. CH_2O concentration then increases at depth 20 cm due to lack of O_2. This effect is also dependent on the consumption of bacteria since there is too much CH_2O concentration in excess at this depth.

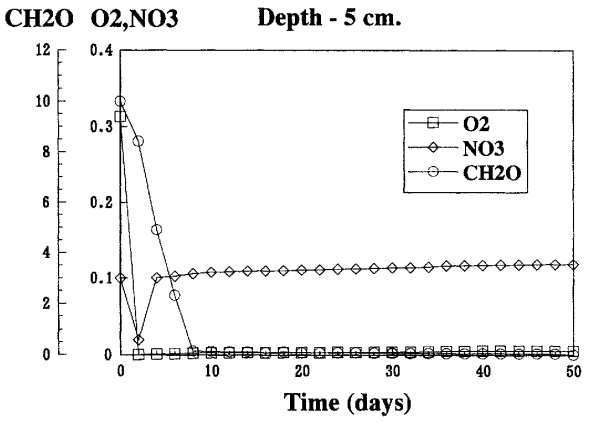

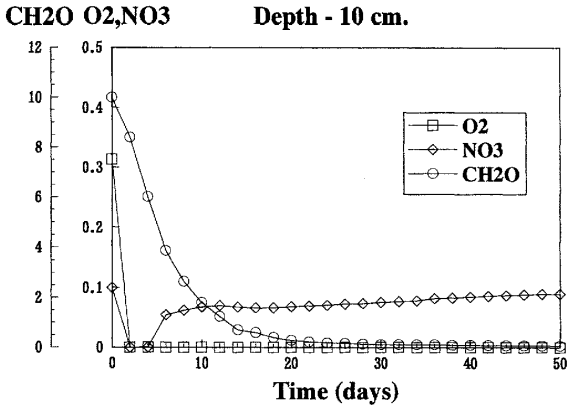

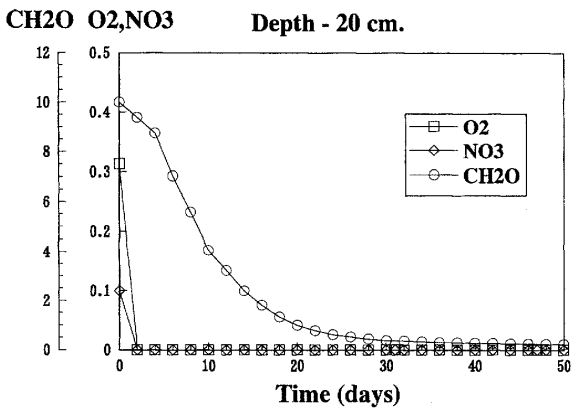

Fig. 14 Mobile redox concentration at different depths with input CH_2O of 0.623 mmol/L and $VK=7.68\times10^{-6}$ cm/sec.

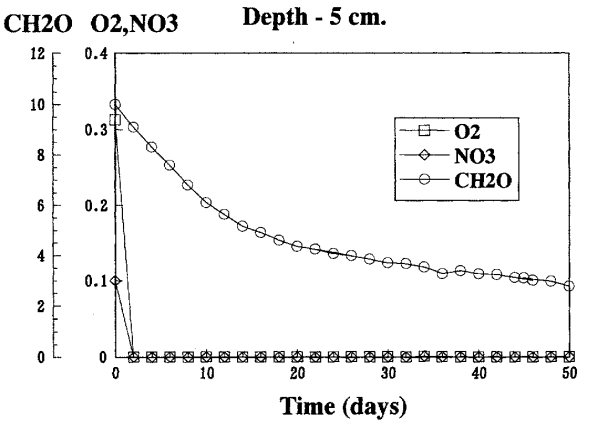

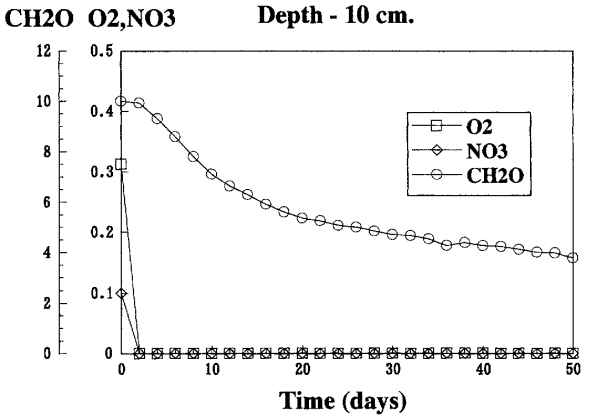

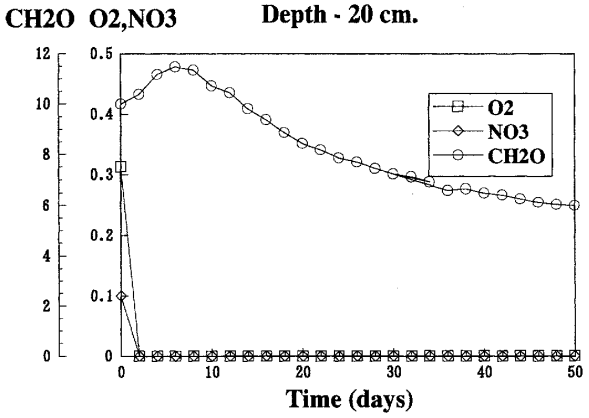

Fig. 15 Mobile redox concentration at different depths with input CH_2O of 62.3 mmol/L and $VK=7.68\times10^{-6}$ cm/sec.

When the input CH_2O in the simulation model is 0.623 mmol/L, NO_3^- concentration infiltrated deeper down to the depths 5 cm and 10 cm of the column. The safe depth of the plow layer in the column, where NO_3^- concentration is totally reduced, can be designed by taking into consideration the input CH_2O concentration at the inject water and velocity of the solute.

Table 7 shows the NO_3^- leach at 10 cm depth in relation to input CH_2O concentration and

Table 7 NO_3^- leach at 10 cm depth in relation to input CH_2O concentration and pore velocity *VK*.

VK /Input CH_2O	CH_2O =0.623 mmol/L	CH_2O = 6.23 mmol/L	CH_2O = 62.3 mmol/L
$VK=7.68\times10^{-6}$ cm/sec	No leach	No leach	No leach
$VK=1.92\times10^{-5}$ cm/sec	No leach	No leach	No leach
$VK=3.84\times10^{-5}$ cm/sec	NO_3^- LEACH	NO_3^- LEACH	No leach

pore velocity *VK*. When *VK* is 7.68×10^{-6} cm/sec and 1.92×10^{-5} cm/sec, the plow layer depth at 10 cm is safe for NO_3^- leach. When $VK=3.84\times10^{-5}$ cm/sec and the input CH_2O concentration is 0.623 mmol/L and 6.23 mmol/L, the plow layer depth at 10 cm is not safe as NO_3^- leach occurred after 4 days. When pore velocity $VK=3.84\times10^{-5}$ cm/sec, higher input CH_2O concentration at inject water is needed so that NO_3^- leach can be prevented.

CH_2O is a significant quantity because the growth of bacteria depends on the presence of CH_2O concentration. The distribution of CH_2O in the soil column and its availability to microorganisms as dissolved organic carbon proved to be a good means to control the distribution of bacteria in the model. In addition, CH_2O also enhances heterotrophic denitrification in which bacteria in anaerobic environment uses NO_3^- as electron acceptor to oxidize dissolved CH_2O. High concentration of CH_2O will result to NO_3^- reduction.

10. Conclusions

The development and use of mathematical models provides a better understanding of the important biological, chemical and hydrological processes relevant to contaminant transport. The multicomponent solute transport model was able to predict the behavior of chemical species present in secondary treated sewage water under redox environment. The observed concentrations correlated fairly well with the simulated concentrations. The model reproduced the sequential reduction reaction. O_2 was reduced first after 30 hours then followed by NO_3^- after 31 hours.

Implementation of wastewater reuse promotes preservation of limited water resources. In designing a wastewater reuse system, it is indispensable to develop an effective treatment scheme that is capable of removing NO_3^- and other contaminants. It is revealed that the multicomponent solute transport model is useful to design the land treatment system for NO_3^- removal from wastewater. CH_2O is a significant quantity because the reduction of NO_3^- and growth of bacteria depend on the presence of CH_2O concentration. When pore velocity *VK* $=7.68\times10^{-6}$ cm/sec and $VK=1.92\times10^{-5}$ cm/sec and input CH_2O concentration are 0.623 mml/L and 6.23 mmol/, the plow layer at depth 10 cm is still safe as NO_3^- concentration was totally reduced. With pore velocity $VK=3.84\times10^{-5}$ cm/sec and input CH_2O concentration at 0.623 mml/L and 6.23 mmol/L, the plow layer at depth 10 cm is unsafe due to NO_3^- concentration increased after 4 days. Since CH_2O can enhance denitrification, lack of CH_2O will cause the NO_3^- to increase again. When the pore velocity is high, higher CH_2O concentration at inject water is needed so that the 10 cm plow layer will be safe. The results show that the multicomponent solute transport model is useful for the description of the biological chemical processes and transport phenomena. Future expansion to two or three dimensions of the model is necessary to address reactive transport at the various scales. Moreover the

influence of the change in hydraulic conductivity due to bacterial growth can be very interesting focus of study in the future.

Acknowledgement

We gratefully acknowledge Prof. Kazutoshi Saeki and Prof. Shinichiro Wada for their contributions and useful comments.

References

1) Appelo, C.A.J., and Willemsen, A. (1987). Geochemical calculations and observation on saltwater intrusions, I. A combined geochemical/mixing cell models, *Journal of Hydrology*, Vol.94, 313-330.
2) Appelo, C.A.J., Willemsen, A., Beekman, H.E. and Griffione, J. (1990). Geochimical calculations and observation on saltwater intrusions, II. Validation of geochemical model with laboratory experiments, *Journal of Hydrology*, Vol.120, 225-250.
3) Appelo, C.A., and Postma, D. (1994). Geochemistry, groundwater and pollution, *A.A. Balkema*, Rotterdam.
4) Bear, J. (1972). Dynamics of Fluid in Porous Media, *American Elsevier*, New York.
5) Bouwer, E.J. and Cobb, G.D. (1987). Modeling of biological processes in the subsurface, *Water Science and Technology*. Vol.19, 769-779.
6) Burden, R.J. (1981). Nitrate contamination of New Zealand aquifers: a review, *New Zealand Journal of Science*, Vol.25, 205-220.
7) Carrera, J., Vicent, T. and Lafuente, F.J. (2003). Influence of temperature on denitrification of an industrial high-strength nitrogen wastewater in a two-sludge system, *Water SA*, Vol.29, 11-16.
8) Dance, J.T. and Reardon, E.J. (1983). Migration of contaminants in groundwater in a landfill: A case study, *Journal of Hydrology*, Vol.63, 109-130.
9) Engesgaard, P. and Christensen, T.H. (1988). A review of chemical solute transport models, *Nordic Hydrology*, Vol.19, 183-216.
10) Frind, E.O., Duynisveld, H.M., Strebel, O., Botcher, J. (1990). Modeling of multicomponent transport with microbial transformation in groundwater: The Furhberg case, *Water Resources Research*, Vol. 26, 1707-1719.
11) Hiroshiro, Y., Jinno, K., Wada, S., Yokoyama, T., and Kubota, M. (1999). Multicomponent solute transport with cation exchange in a redox subsurface environment, *Calibration and Reliability in Groundwater Modeling* (Proceedings of the ModelCARE 99 conference held at Zurich, 1999), 474-480.
12) Hiroshiro, Y., Jinno K., Yokoyama, T. and Wada S.I. (1999). Behaviour of chemical species under reducing condition in a subaqueous soils column, *Lowland Technology International*, Vol.1, pp. 59-66.
13) Kindred, J.S. and Celia, M.A. (1989). Contaminant transport and biodegradation 2. Conceptual model and test simulations, *Water Resources Research*, Vol.256, 1149-1159.
14) Kinzelbach, W. and Schäfer, W. (1989). Coupling of chemistry and transport, Groundwater Management, *IAHS Publications*, Vol.188, 237-259.
15) Kinzelbach, W., Schäfer, W. and Herzer, J. (1991). Numerical modeling of natural and enhanced denitrification processes in aquifer, *Water Resources Research*, Vol.27(6), 1123-1135.
16) Kubota, M., Hiroshiro, Y., Jinno, K., Yokoyama, T. and Wada, S.I. (1998). Properties of

multicomponent transport in a subsurface environment, Proceedings of the International Symposium on Lowland Technology/Saga University, 487-494.
17) Lance, J.C. and Gerba, C.P. (1977). Nitrogen, phosphate and virus removal from sewage water during land filtration, *Progressive Water Technology*, Vol.9, 157-166.
18) Lensing, H.J., Vogt, M. and Herrling, B. (1994). Modeling of biologically mediated redox processes in the subsurface, *Journal of Hydrology*, Vol.159, 125-143.
19) Liu, C.W. and Narasimhan, T.N. (1989a). Redox-controlled multiple species reactive chemical transport I. Model development, *Water Resources Research*, Vol.25(5), 869-882.
20) Liu, C.W. and Narasimhan, T.N. (1989b). Redox-controlled multiple species reactive chemical transport I. Verification and application, *Water Resources Research*, Vol.25(5), 883-910.
21) Mac Quarrie, K.T.B. and Sudicky, E.A. (2001). Multicomponent simulation of wastewater derived nitrogen and carbon in shallow unconfined aquifers I. Model formulation and performance, *Journal of Contaminant Hydrology*, Vol.47, 53-84.
22) Mac Quarrie, K.T.B., Sudicky, E.A. and Robertson, W.D. (2001). Numerical simulation of fine-grained denitrification layer for removing septic system nitrate from shallow groundwater, *Journal of Contaminant Hydrology*, Vol.52, 29-55.
23) Mc Nab, W.W. and Nasarimhan, T.N. (1994). Modeling reactive transport of organic compounds in groundwater using partial redox disequilibrium approach, *Water Resources Research*, Vol.30, 2619-2635.
24) Miller, C.W. and Benson, L.V. (1983). Simulation of solute transport in a chemical reactive heterogeneous system: model development and application, *Water Resources Research*, Vol.19, 381-391.
25) Molz, F.J., Widdowson, M.A. and Benefield, L.D. (1986). Simulation of microbial growth dynamics coupled to nutrient and oxygen transport in porous media, *Water Resources Research*, Vol.22, pp.1207-1216.
26) Momii, K., Hiroshiro, Y., Jinno, K. and Berndtsson, R. (1997). Reactive solute transport with a variable selectivity coefficient in an undisturbed soil column, *Soil Science Society of America Journal*, Vol.61(6), 1539-1546.
27) Polprasert, C. (1996). Organic Waste Recycling, *John Wiley and Sons Inc.*, London.
28) Postma, D., Boesen, C., Kristiansen, H., and Larsen F. (1991). Nitrate reduction in an unconfined sandy aquifer: water chemistry, reduction processes and geochemical modeling, *Water Resources Research*, Vol.27(8), 2027-2045.
29) Schäfer, W. and Therrien R. (1995). Simulating transport and removal of xylene during remediation of a sandy aquifer, *Journal of Contaminant Hydrology*, Vol.19, 205-236.
30) Schäfer, D., Schäfer, W. and Kinzelbach, W. (1998). Simulation of reactive processes related to biodegradation in aquifers 1. Structure of the three-dimensional reactive transport model, *Journal of Contaminant Hydrology*, Vol.31, 167-186.
31) Schulz, H.D. and Reardon, E.J. (1983). A combined mixing cell/analytical model to describe two-dimensional reactive solute transport for unidirectional groundwater flow, *Water Resources Research*, Vol.19, 493-502.
32) Stumm, W. and Morgan J.J. (1981). Aquatic Chemistry, *John Wiley & Sons Inc.*, New York.
33) Trudell, M.R., Gillham, R.W. and Cherry J.A. (1986). An in-situ study of the occurrence and rate of denitrification in a shallow unconfined sand aquifer, *Journal of Hydrology*, Vol.83, 251-268.
34) Vallochi, A.J., Street, R.L. and Roberts, P.V. (1981). Transport of Ion-exchanging solutes in groundwater: chromatographic theory and field simulation, *Water Resources Research*,

Vol.17, 1517-1527.
35) Von Gunten, U. and Zobrist, J. (1993). Biogeochemical changes in groundwater infiltration systems: columns studies, *Geochim Cosmochim Acta*, Vol.57, 3895-3906.
36) Widdowson, M.A., Molz, F.J. and Benefield, L.D. (1988). A numerical transport model for oxygen- and nitrate-based respiration linked to substrate and nutrient availability in porous media, *Water Resources Research*, Vol.24(9), 1553-1565.
37) Zheng, Z. and Bennet, G.D., (1995): Applied Contaminant Transport: Modelling, Theory and Practice, *Van Nostrand Reinhold*, New York.